A&A 642, A16 (2020)
https://doi.org/10.1051/0004-6361/201937259

Astronomy & Astrophysics
Special issue

The Solar Orbiter mission

The Solar Orbiter Solar Wind Analyser (SWA) suite

C. J. Owen[1], R. Bruno[2], S. Livi[3], P. Louarn[4], K. Al Janabi[1], F. Allegrini[3], C. Amoros[4], R. Baruah[4], A. Barthe[4], M. Berthomier[5], S. Bordon[4], C. Brockley-Blatt[1], C. Brysbaert[6], G. Capuano[7], M. Collier[8], R. DeMarco[2], A. Fedorov[4], J. Ford[3], V. Fortunato[9], I. Fratter[6], A. B. Galvin[10], B. Hancock[1], D. Heirtzler[10], D. Kataria[1], L. Kistler[10], S. T. Lepri[11], G. Lewis[1], C. Loeffler[3], W. Marty[4], R. Mathon[4], A. Mayall[1], G. Mele[12], K. Ogasawara[3], M. Orlandi[13], A. Pacros[14], E. Penou[4], S. Persyn[3], M. Petiot[4], M. Phillips[3], L. Přech[15], J. M. Raines[11], M. Reden[16], A. P. Rouillard[4], A. Rousseau[1], J. Rubiella[4], H. Seran[4], A. Spencer[1], J. W. Thomas[11], J. Trevino[3], D. Verscharen[1,10], P. Wurz[24], A. Alapide[12], L. Amoruso[9], N. André[4], C. Anekallu[1], V. Arciuli[13], K. L. Arnett[11], R. Ascolese[7], C. Bancroft[10], P. Bland[3], M. Brysch[3], R. Calvanese[7], M. Castronuovo[21], I. Čermák[17], D. Chornay[8], S. Clemens[11], J. Coker[1], G. Collinson[8], R. D'Amicis[2], I. Dandouras[4], R. Darnley[1], D. Davies[1,†], G. Davison[1], A. De Los Santos[3], P. Devoto[4], G. Dirks[3], E. Edlund[3], A. Fazakerley[1], M. Ferris[3], C. Frost[10], G. Fruit[4], C. Garat[4], V. Génot[4], W. Gibson[3,†], J. A. Gilbert[11], V. de Giosa[12], S. Gradone[1], M. Hailey[1], T. S. Horbury[18], T. Hunt[1], C. Jacquey[4], M. Johnson[3], B. Lavraud[4], A. Lawrenson[1], F. Leblanc[5], W. Lockhart[3], M. Maksimovic[19], A. Malpus[1], F. Marcucci[2], C. Mazelle[4], F. Monti[7], S. Myers[3], T. Nguyen[3], J. Rodriguez-Pacheco[20], I. Phillips[1], M. Popecki[10,25], K. Rees[1], S. A. Rogacki[11], K. Ruane[1], D. Rust[1], M. Salatti[21], J. A. Sauvaud[4], M. O. Stakhiv[11], J. Stange[3], T. Stubbs[8], T. Taylor[3], J.-D. Techer[5], G. Terrier[4], R. Thibodeaux[3], C. Urdiales[3], A. Varsani[1], A. P. Walsh[22], G. Watson[1], P. Wheeler[1], G. Willis[1], R. F. Wimmer-Schweingruber[23], B. Winter[1], J. Yardley[1], and I. Zouganelis[22]

(Affiliations can be found after the references)

Received 5 December 2019 / Accepted 8 July 2020

ABSTRACT

The Solar Orbiter mission seeks to make connections between the physical processes occurring at the Sun or in the solar corona and the nature of the solar wind created by those processes which is subsequently observed at the spacecraft. The mission also targets physical processes occurring in the solar wind itself during its journey from its source to the spacecraft. To meet the specific mission science goals, Solar Orbiter will be equipped with both remote-sensing and in-situ instruments which will make unprecedented measurements of the solar atmosphere and the inner heliosphere. A crucial set of measurements will be provided by the Solar Wind Analyser (SWA) suite of instruments. This suite consists of an Electron Analyser System (SWA-EAS), a Proton and Alpha particle Sensor (SWA-PAS), and a Heavy Ion Sensor (SWA-HIS) which are jointly served by a central control and data processing unit (SWA-DPU). Together these sensors will measure and categorise the vast majority of thermal and suprathermal ions and electrons in the solar wind and determine the abundances and charge states of the heavy ion populations. The three sensors in the SWA suite are each based on the top hat electrostatic analyser concept, which has been deployed on numerous space plasma missions. The SWA-EAS uses two such heads, each of which have 360° azimuth acceptance angles and ±45° aperture deflection plates. Together these two sensors, which are mounted on the end of the boom, will cover a full sky field-of-view (FoV) (except for blockages by the spacecraft and its appendages) and measure the full 3D velocity distribution function (VDF) of solar wind electrons in the energy range of a few eV to ~5 keV. The SWA-PAS instrument also uses an electrostatic analyser with a more confined FoV (−24° to +42° × ±22.5° around the expected solar wind arrival direction), which nevertheless is capable of measuring the full 3D VDF of the protons and alpha particles arriving at the instrument in the energy range from 200 eV/q to 20 keV/e. Finally, SWA-HIS measures the composition and 3D VDFs of heavy ions in the bulk solar wind as well as those of the major constituents in the suprathermal energy range and those of pick-up ions. The sensor resolves the full 3D VDFs of the prominent heavy ions at a resolution of 5 min in normal mode and 30 s in burst mode. Additionally, SWA-HIS measures 3D VDFs of alpha particles at a 4 s resolution in burst mode. Measurements are over a FoV of −33° to +66° × ±20° around the expected solar wind arrival direction and at energies up to 80 keV/e. The mass resolution ($m/\Delta m$) is >5. This paper describes how the three SWA scientific sensors, as delivered to the spacecraft, meet or exceed the performance requirements originally set out to achieve the mission's science goals. We describe the motivation and specific requirements for each of the three sensors within the SWA suite, their expected science results, their main characteristics, and their operation through the central SWA-DPU. We describe the combined data products that we expect to return from the suite and provide to the Solar Orbiter Archive for use in scientific analyses by members of the wider solar and heliospheric communities. These unique data products will help reveal the nature of the solar wind as a function of both heliocentric distance and solar latitude. Indeed, SWA-HIS measurements of solar wind composition will be the first such measurements made in the inner heliosphere. The SWA data are crucial to efforts to link the in situ measurements of the solar wind made at the spacecraft with remote observations of candidate source regions. This is a novel aspect of the mission which will lead to significant advances in our understanding of the mechanisms accelerating and heating the solar wind, driving eruptions and other transient phenomena on the Sun, and controlling the injection, acceleration, and transport of the energetic particles in the heliosphere.

Key words. instrumentation: detectors – plasmas – Sun: heliosphere – solar wind – Sun: particle emission

† Deceased.

1. Introduction

Solar Orbiter was formally selected by the European Space Agency (ESA) on October 4, 2011 to fill the first launch slot for "medium" class missions under the agency's "Cosmic Vision 2015−2025" programme. The mission, formally a collaboration between ESA and NASA, has top-level science goals which are centred on understanding how our Sun creates and controls the heliosphere, that is the volume of ionised material forming a "bubble" in interstellar space in which all of the planets of our Solar System reside.

As detailed elsewhere in this volume (e.g. Müller et al. 2020), and, for example, in Müller et al. (2013), the primary, overarching scientific objective above can be broken down into four inter-related scientific questions, all of which have strong, direct relevance to the Cosmic Vision theme "How does the Solar System work?". The four top-level scientific questions that will be addressed by Solar Orbiter, each together with three key targeted sub-questions, are as follows:

1. How and where do the solar wind plasma and magnetic field originate in the corona?
   - What are the source regions of the solar wind and heliospheric magnetic field?
   - What mechanisms heat and accelerate the solar wind?
   - What are the sources of solar wind turbulence and how does it evolve?
2. How do solar transients drive heliospheric variability?
   - How do coronal mass ejections (CMEs) evolve through the corona and inner heliosphere?
   - How do CMEs contribute to solar magnetic flux and helicity balance?
   - How and where do shocks form in the corona?
3. How do solar eruptions produce energetic particle radiation that fills the heliosphere?
   - How and where are energetic particles accelerated at the Sun?
   - How are energetic particles released from their sources and distributed in space and time?
   - What are the seed populations for energetic particles?
4. How does the solar dynamo work and drive connections between the Sun and the heliosphere?
   - How is magnetic flux transported to and re-processed at high solar latitudes?
   - What are the properties of the magnetic field at high solar latitudes?
   - Are there separate dynamo processes acting in the Sun?

These are currently fundamental open questions in solar and heliophysics. By addressing them with the observations made by the Solar Orbiter mission, major breakthroughs in our understanding of how the inner Solar System works, and how it is driven by solar activity, will be made.

To answer these questions, it is essential, in coordination with other observations, to make in-situ measurements of the solar wind plasma close enough to the Sun that it is still relatively pristine and has not had its properties modified by subsequent transport and propagation processes. This is one of the fundamental drivers for the Solar Orbiter mission, which will approach the Sun to distances as close as ∼0.28 AU. In addition, measurement of the solar wind plasma at high solar latitudes (several tens of degrees outside of the ecliptic) is also a primary driver for the mission. Making these critical measurement of the thermal and suprathermal components of the plasma population, including electrons, protons, alpha particles, and the minor heavy ion constituents, is the responsibility of the Solar Wind Analyser (SWA) suite of sensors, which is specifically detailed in this paper. The in-situ measurements of solar wind plasma made by SWA, together with those of the Magnetic fields and Radio and Plasma Wave instruments (MAG and RPW, Horbury et al. 2020; Maksimovic et al. 2020, both this issue, respectively), and the Energetic Particle Detector suite (EPD, Rodríguez-Pacheco et al. 2020) form a coherent description of the state of the solar wind local to the spacecraft. These measurements will be traced back to the source regions and structures on the Sun which can be observed using simultaneous, high-resolution imaging and spectroscopic measurements of the Sun, both in and out of the ecliptic plane, by the complement of remote sensing instruments (Auchère et al. 2020, and references therein) within the Solar Orbiter payload. The resulting combination of in-situ and remote sensing instruments on the same, purpose-built spacecraft (García-Marirrodriga et al. 2020), together with the new, inner-heliospheric perspective, distinguishes Solar Orbiter from all previous and current missions. This will enable breakthrough science which can be achieved in no other way.

We note also that the science goals of the Solar Orbiter mission are increasingly relevant to society, in that our own planet orbits within the heliospheric "bubble" and is subject to major disruptions to its near-space environment, which are of solar origin. Thus the mission not only promises to advance the fields of solar and heliospheric physics in their own right, but will make great progress on understanding the physics behind "space weather" and its impact on our technological society.

2. Requirements and expected results

2.1. Primary science motivations

The overarching objective of SWA is to provide the comprehensive in situ measurements of the solar wind which are critical if we are to establish the fundamental physical links between the Sun's highly dynamic and inhomogeneous magnetised atmosphere and the solar wind in all its quiet and disturbed states. This critical step requires comprehensive in-situ measurements of the various constituents of the solar wind plasma including high-time resolution velocity distributions of solar wind electrons and ions and composition up to suprathermal energies. These measurements are vital if we are to discover the fundamental links between, for example, solar eruptions, shocks and the suprathermal ions that are the seed populations of hazardous solar particle events.

The moments (i.e. density, bulk velocity, temperature, etc.) of the electron and proton VDFs provide the crucial information to link the global evolution of the solar wind to its local in-situ properties. These parameters characterise the solar-wind plasma that convects structures over the spacecraft. They also describe the medium through which CMEs and energetic particles propagate, making their measurement critical for the understanding of the evolution of these events. Therefore, the characterisation of the plasma environment around the spacecraft, in which it takes all in-situ measurements, heavily relies on knowledge of the plasma moments.

In addition to this general motivation for measuring the plasma environment, detailed knowledge of the particle properties will support Solar Orbiter's goal to link the coronal source regions with the in-situ solar wind. One such example is the electron strahl, a magnetic field-aligned beam of suprathermal electrons in the electron VDF, which usually propagates in the anti-Sunward direction (Feldman et al. 1975; Pilipp et al. 1987).

The orientation and density of the electron strahl are predictive tools to study the magnetic connectivity of the spacecraft with the solar corona (Steinberg et al. 2005; Owens et al. 2008, 2017). Furthermore, the ability to link solar wind to its solar sources is greatly enhanced by the inclusion of heavy ion measurements of both the ionic and elemental composition of solar wind plasma. Solar wind ion composition is determined by the electron density, temperature, and residence time in the ionising region during the solar wind's release from the low corona, usually freezing-in within 5 Solar radii (R_S) (Hundhausen et al. 1968; Gloeckler et al. 2003; Zurbuchen et al. 2002; Zurbuchen 2007; Ko et al. 1997; Landi et al. 2012). The fact that the ion composition is set within 5 R_S and remains unchanged during its transit through the heliosphere makes it a powerful tool for linking the solar wind to coronal source regions (Zurbuchen et al. 2002; Zhao et al. 2009; Landi et al. 2012). In addition, heavy ion elemental abundances are determined by processes in the chromosphere that can preferentially draw low first ionisation potential (FIP) ions up into closed fields in the corona for later release into the solar wind (e.g. see Laming 2015). Hence, different sources of solar wind (e.g. coronal holes vs. quiet Sun regions with initially closed fields) exhibit different enhancements in ions with low FIP, making elemental abundance measurements indicators of these sources (Feldman & Widing 2003; Zurbuchen et al. 1999, 2002; von Steiger et al. 2001). Combining measurements from SWA with SPICE (SPICE Consortium 2020), which remotely measures the ionisation of the corona will provide the most powerful set of measurements to date for linking the corona to the heliosphere.

By way of example of the contributions that SWA will make, we note that during intervals around perihelion, SWA will measure the solar wind plasma (electrons and ions) in magnetic flux tubes that can be readily traced back to their solar source regions, whose morphology, structure, and variability can be determined from Solar Orbiter's simultaneous remote-sensing observations. These sources can be observed over an extended period, compared to that available from Earth, and the observations will allow us to resolve outstanding questions about the origins of fast and slow wind, the distribution of open magnetic flux, the sources of solar wind turbulence and its dissipation to heat, and accelerate the wind (see Fig. 1). For example, the combined data set will allow us to determine how the nature of the fast solar wind relates to the 3D structure of coronal holes, whether the slow solar wind originates from the over-expanded edges of coronal holes or coronal loops outside of coronal holes. The measurements will help determine the distribution of open magnetic flux and the near-Sun drivers of solar wind turbulence.

Transient events such as CMEs and interplanetary shocks are characterised by rapid changes in the plasma parameters. Measurements by the SWA suite will facilitate studies of the evolution of plasma within these structures in unprecedented detail. For example, SWA measurements will advance our understanding of CME structure, the physical mechanisms of CME initiation, and the global influence of CMEs on the coronal and heliospheric magnetic fields. SWA measurements will provide tests of CME initiation, by utilising plasma signatures to differentiate between models (e.g. Lynch et al. 2011; Reinard et al. 2012), and will allow us to assess the impacts of CMEs on the magnetic configuration of the inner heliosphere. As Solar Orbiter traverses the inner heliosphere, approaching distances as close as 60 R_S from the Sun, SWA will measure the structure and evolution of shocks and other small-scale transients.

The particle VDFs in the solar wind often show deviations from the Maxwellian equilibrium state (Marsch 2006). These

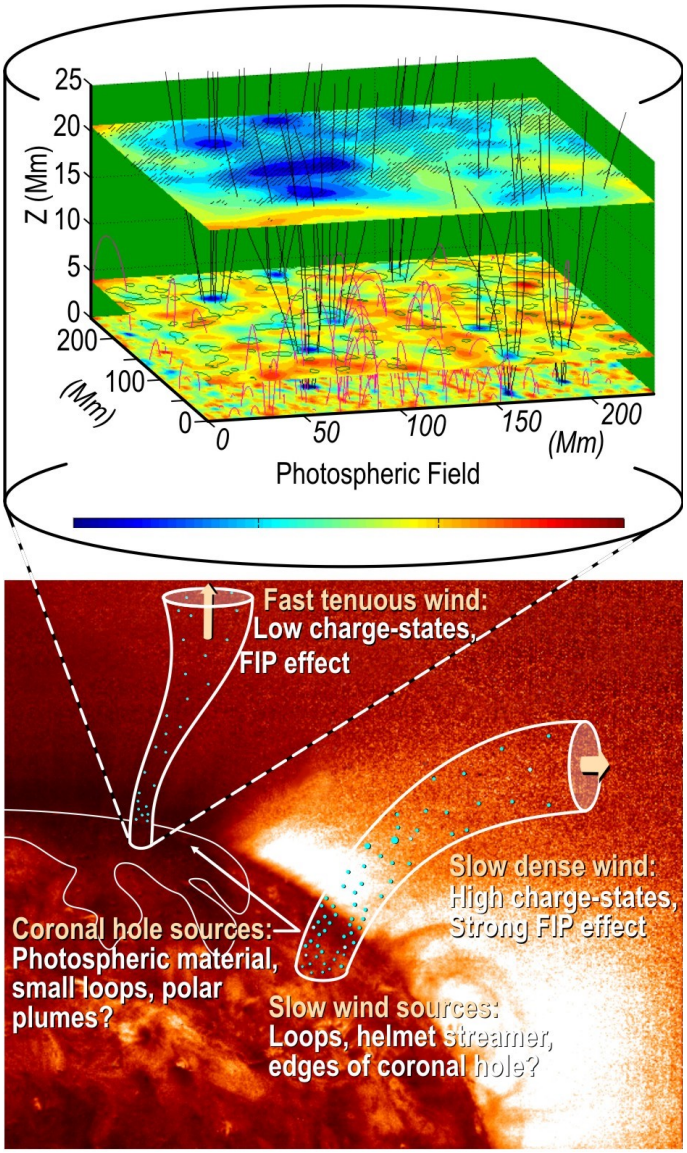

Fig. 1. Central goals of Solar Orbiter. These are to establish the physical links between the observed solar wind and its sources back on the Sun. The illustration shows some of the observed properties of fast wind from coronal holes and slow wind that may emanate from coronal hole edges, from loops beyond the coronal or the helmet streamer. The cut-out shows the complex magnetic structure modelled at the base of a fast wind flux tube that rapidly expands out of the chromosphere and into the corona. Understanding the dynamics of the solar magnetic atmosphere, and its signatures in the measured solar wind holds the key to understanding the sources of all solar wind (adapted from Tu et al. 2005; Schwadron & McComas 2003).

features are the result of a complex interplay between coronal heating, acceleration, global expansion, and local kinetic processes and thus give insight into the processes that determine the evolution of the solar wind plasma. Since the particle VDFs describe the local plasma thermodynamics at the spacecraft completely, the understanding of the solar wind thermodynamics and evolution requires that the particle VDFs, including their non-Maxwellian features, be measured and linked to the electromagnetic fields in the plasma in great detail and at high cadence and resolution. SWA will measure the kinetic microstate of the solar wind by measuring full 3D distributions and, at a higher cadence, 2D pitch-angle distributions of the plasma ions and electrons.

Non-equilibrium features in each particle species play a unique and prominent role. For example, the kinetic structure of the electron distribution is important for the global heat conduction in the plasma, while the kinetic structure of the ion distributions reflects momentum and energy transfer processes such as local heating and kinetic instabilities. These aspects of the solar wind particle distributions show a distinct evolution with heliocentric distance, latitude, and longitude (Verscharen et al. 2019). Solar wind internal energy is shared between all ions and electrons by wave-particle interactions, turbulence, and weak but unavoidable Coulomb collisions. Small-scale kinetic processes also act together with large-scale fluid processes in the acceleration of particles at reconnection sites and shocks. The comprehensive SWA sensor suite, with its novel observational strategy exploiting the Solar Orbiter orbital characteristics, will investigate the cross-scale couplings that constitute the Sun-heliosphere connections (Verscharen et al. 2019), from the global magnetohydrodynamic scales down to the local kinetic scales of wave-particle interactions in the solar wind.

If the non-equilibrium features in the VDF become large enough, the system will drive kinetic micro-instabilities that create small-scale electromagnetic fluctuations on which the particles scatter (Gary 1993). This scattering process reduces the deviation from equilibrium by bringing the shape of the VDF closer towards equilibrium. Known non-equilibrium features that drive instabilities include temperature anisotropies (Gary et al. 1976; Gary & Karimabadi 2006; Hellinger et al. 2006; Bale et al. 2009), ion beams (Gary et al. 1984; Gary 1991), differential streaming between protons and alpha particles (Gary et al. 2000; Verscharen et al. 2013), and electron heat flux (Gary et al. 1975; Verscharen et al. 2019), amongst others. Instabilities are important mechanisms for the overall thermodynamics of the plasma (Matteini et al. 2013; Verscharen et al. 2015; Yoon & Sarfraz 2017; Stansby et al. 2019). Therefore, the detailed study of non-equilibrium features that potentially drive instabilities and the search for the signatures that result from the action of instabilities are necessary to understand the impact of these micro-instabilities on the evolution of the solar wind. SWA will deliver on both of these requirements.

Measurements of the particle VDFs are also a critical component for the interpretation of the ubiquitous turbulent fluctuations in the solar-wind plasma. These fluctuations are characterised by self-consistent interactions between the fields and the particles. Therefore, the observation of the fluctuations in the particle VDF will give us insight into the nature of the turbulent fluctuations in general (Šafránková et al. 2019; Wu et al. 2019). Furthermore, the secular transfer of energy from the turbulent fluctuations into particle heating creates characteristic signatures in the velocity distribution such as the formation of quasi-linear plateaus through cyclotron-resonant and Landau-resonant dissipation (Dusenbery & Hollweg 1981; Marsch et al. 1982, 2003; Isenberg & Hollweg 1983) or flattening of the core of the distribution through stochastic heating (Klein & Chandran 2016). Finding these signatures in the velocity distributions will improve our understanding of the nature of the turbulent fluctuations and the relevant dissipation processes. These measurements of turbulent fluctuations in the VDFs and their moments require a high cadence in order to resolve small-scale fluctuations (Nicolaou et al. 2019) and a high resolution in order to resolve the characteristic signatures of heating. SWA will provide sufficient cadence and resolution to perform these studies.

Instabilities, turbulence, and other kinetic plasma processes result from, and participate in, a complex interplay between interactions in the solar-wind source regions, the large-scale expansion of the solar wind, and local plasma physics. These energy-transfer mechanisms have a strong impact on the thermodynamics and evolution of the solar wind and are thus important for our understanding (Verscharen et al. 2019). The radial evolution of turbulence and the continuous heating of the fast wind are clear examples of this kind of dynamical processes. SWA will measure the in-situ signatures of these processes mainly through provision of high-resolution solar wind VDFs. These distributions will show kinetic features like the electron strahl, ion temperature anisotropies, and differential streaming, which are most likely the results of a combination of local wave-particle interactions (near the Sun or in the solar wind) and global expansion effects.

The thermal and suprathermal particles in the solar wind also serve as part of the seed population for the acceleration of energetic particles through transient events such as interplanetary shock waves. Therefore, understanding the kinetic properties of these seed particles is important for the development of a better understanding of the production of energetic particle radiation in the inner heliosphere. SWA will characterise these particles completely down to kinetic scales, for example to determine the sources and acceleration mechanisms of the so-called large gradual solar energetic particle (SEP) events and determine the properties, composition, and evolution of suprathermal ions that seed these higher-energy particles.

During later phases of the mission, Solar Orbiter measurements will reveal the latitudinal dependence of these phenomena as the spacecraft climbs out of the ecliptic. Moreover, as the orbit repeatedly covers a range of heliocentric distances, the in situ instruments will also provide key information on the evolution of the solar wind with distance from the Sun, providing a separation of those processes which are inherent in the solar wind itself from those which play a role in the formation of the young, "pristine" wind near to the Sun. Solar Orbiter will thus extend our direct measurements of space plasmas into a new realm that will transform our view of the connections from the solar atmosphere into the solar wind, and help us project this understanding to other stellar environments.

2.2. General overview of SWA measurement requirements

The Solar Orbiter science goals, as expressed above, can only be achieved with the inclusion of a SWA-like package within the Solar Orbiter payload to provide moments and VDFs of electrons and ions. Indeed, measurements of the kind made by SWA are required for all of the mission science goals (Müller et al. 2013, 2020; Zouganelis et al. 2020). They are also fundamental to supporting modelling and analysis of the Sun-spacecraft connection (Rouillard et al. 2020), and multi-mission science opportunities requiring observations from more dispersed perspectives, such as those which will be achieved with Parker Solar Probe (Velli et al. 2020).

Electrons, protons, and alpha particles are the most abundant populations of the solar and heliospheric plasma. The electron strahl in the solar wind is generally the fastest of these plasma populations and thus provides the early information on any processes happening remotely from the spacecraft. The electron, proton, and heavy-ion VDFs with their moments and their typical non-Maxwellian features must be fully resolved by the SWA sensors, in order to provide critical information on the plasma globally and locally, its large-scale thermodynamics, its remote sources on the Sun, and furthermore about the transport processes (e.g. instabilities and turbulence) in operation between these sources and the spacecraft location. The compositional

signatures which must be measured by SWA are necessary to provide clearer constraints for theories on the origin of solar wind streams, and in particular of CMEs. For example, the kinetic properties of the heavy ions are required to provide information about the non-thermal processes heating the plasma and accelerating the solar wind. The ionic charge states of the local plasma must also be of sufficient quality to enable direct comparison with the remote observations of the coronal plasma., such that elemental and compositional signatures can be related to ultraviolet diagnostics of the solar source regions from remote-sensing observations.

SWA must consist of a suite of sensors that are able to measure the 3D VDFs of the major solar wind constituents: electrons, protons, and alpha particles. The basic moments of the distributions, such as density, velocity, pressure tensor, and heat flux vector must be obtained under all solar wind conditions and must be sampled with sufficient cadence to characterise fully the fluid and kinetic state of the wind. In addition, measurements supporting the derivation of relative elemental abundances, ionic charge state ratios and distributions, velocity space distributions and moments (population density, bulk flow speed and temperature) of representative high-FIP elements (the C, N, O group), and of low-FIP elements (such as Fe, Si or Mg) are required. These measurement challenges provide the motivation for our instrument suite comprising three distinct sensors:

– The Electron Analyser System (SWA-EAS) to measure the VDFs of electrons (including core, halo, and strahl electrons) and their moments at high time resolution;

– The Proton-Alpha Sensor (SWA-PAS) to measure the VDFs of major ion species and their moments at high time resolution and determine their moments;

– The Heavy Ion Sensor (SWA-HIS) to measure the VDFs of prominent minor ion species and determine their abundances and charge states.

To fully address the Solar Orbiter science goals, the SWA-EAS must resolve the full 3D velocity space distributions of solar wind electrons with high cadence (<10 s time resolution). Since the electron thermal velocity is much greater than their bulk velocity, the electrons arrive at the spacecraft from all directions. Therefore, even in the solar wind, such a measurement of the 3D electron VDF can only be achieved by a sensor (or a set of sensors) that has a combined FoV covering a large fraction of the full sky. In addition, the sensor is required to provide 2D pitch angle distributions (PADs) with high time resolution (ideally at a cadence of 0.125 s). Data from MAG (Horbury et al. 2020) are used onboard to determine the orientation of the magnetic field, which is necessary to produce the PADs and is thus required at this high cadence. The specific design goals for SWA-EAS, based on these general requirements, are presented in Sect. 3.1.6.

Fully addressing the Solar Orbiter science questions also requires the SWA-PAS sensor to be capable of resolving the full 3D VDFs of solar wind protons and alpha particles with high cadence (<10 s time resolution), as well as measuring the bulk plasma parameters (i.e. the moments) at ultra-high time resolution (as fast as ~0.1 s) to characterise the global structure and dynamics of the 3D inner heliosphere and improve our basic understanding of the kinetic processes, microstate, instabilities, and turbulence in the evolving solar wind from ~0.28−1.0 AU. The SWA-PAS energy coverage and resolution, FoV, angular coverage and resolution, geometric factor, and time resolution must be such that it can measure solar wind protons and alpha particles for more than 99% of the time during the Solar Orbiter mission profile. The specific design goals for SWA-PAS, based on these general requirements, are presented in Sect. 3.3.6.

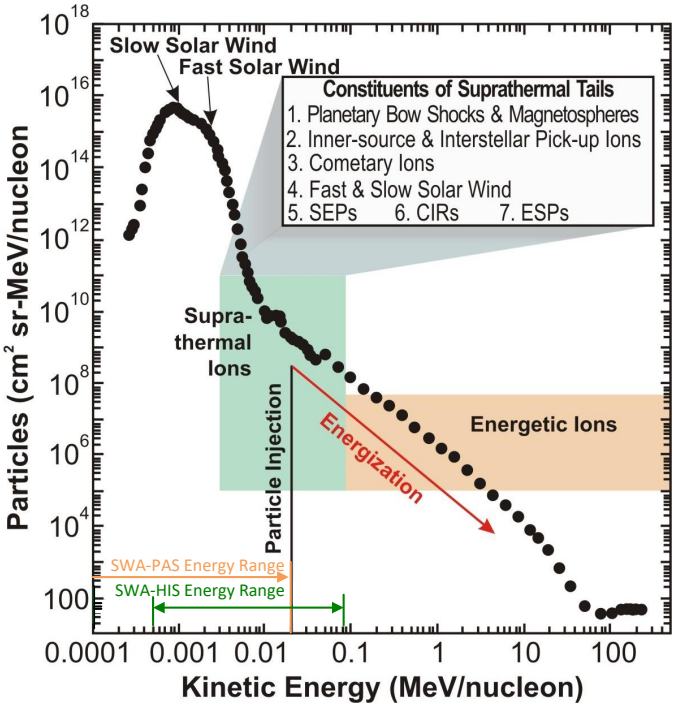

Fig. 2. SWA measurement range for the ion composition and energy distribution extending from the solar wind into the suprathermal domain and covering the energy range of SEP seed particles injected to shock acceleration (adapted from Mewaldt et al. 2003; shown here are oxygen fluences from ACE measured over a 3-year period). SWA-PAS and SWA-HIS energy ranges are shown at the bottom of the figure for comparison.

Finally, the SWA-HIS must address two fundamentally different sets of measurement objectives. First, SWA-HIS must measure the composition and 3D VDFs of heavy ions in the bulk solar wind as well as that of pick-up ions. Second, SWA-HIS must measure the composition and 3D VDFs of the major constituents in the suprathermal energy range (see Fig. 2). The sensor must be able to resolve the full 3D VDFs of the prominent heavy ions at a resolution of 5 min in normal mode and 30 s in burst mode. Additionally, SWA-HIS must measure 3D VDFs of alpha particles at 4 s resolution in burst mode. Measurements must be made up to 60 keV/e, with mass resolution ($m/\Delta m$) of ~5. These will be the first such measurements in the inner heliosphere. The specific design goals for SWA-HIS, based on these general requirements, are presented in Sect. 3.2.6.

In summary, the measurements by the SWA suite are central to addressing critical parts of the Solar Orbiter top-level science questions related to the in situ solar wind, the connectivity between the spacecraft, the wind's coronal source regions, and suprathermal ion populations throughout the heliosphere. Through its capability of measuring the 3D VDFs of electrons and ions, SWA is a pivotal and indispensable instrument suite for establishing the links between processes remotely observed in the corona and the resulting heliospheric plasma properties measured in situ, and for revealing their complex multiple connections.

3. SWA sensor descriptions

In this section we provide a summary of the technical details of each of the four hardware elements that comprise the SWA suite. For each of the three scientific sensors, we provide an

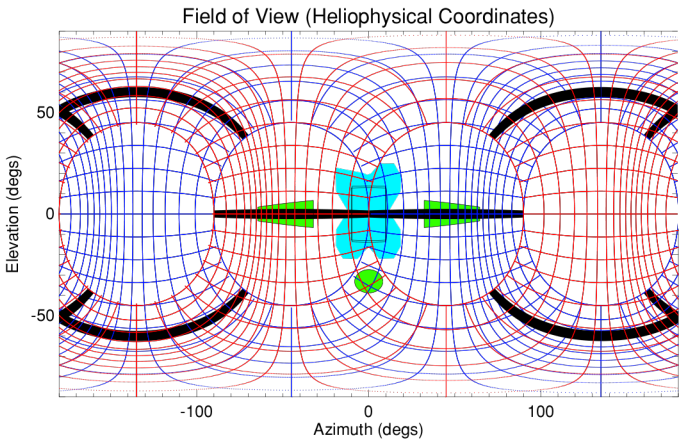

Fig. 3. Expected combined FoV for the 2-head SWA-EAS unit. The figure covers the full sky (±90° in elevation and ±180° in azimuth), with the blue grid indicating the regions of sky sampled by SWA-EAS1 and the red grid that sampled by SWA-EAS2. The black bars indicate regions of the sky occluded by sensor structure, in this case the three support pillars on each sensor which are clearly visible in Fig. 4. The green shaded regions indicate the approximate projection of spacecraft appendages in the FoV, namely the solar arrays and the high gain antenna. The blue shaded region indicates the blockage to the FoV due to a boom-mounted baffle designed to shield the instrument from direct impingement of thruster exhausts. (The relative projection of the spacecraft itself is indicated by the rectangle within this latter region).

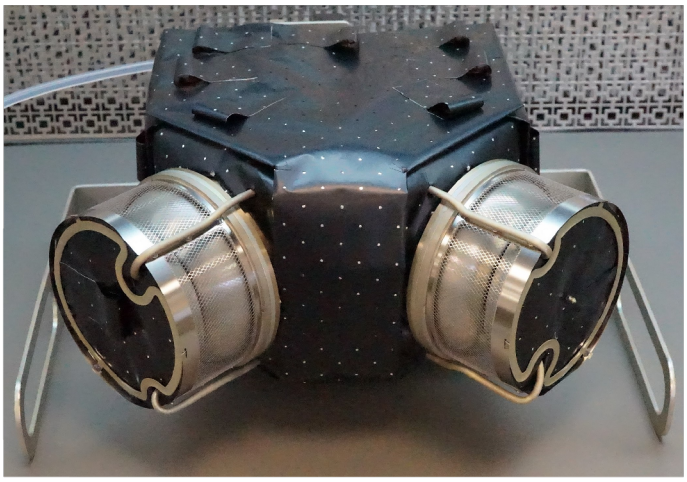

Fig. 4. Flight model of the SWA-EAS unit, showing the two orthogonally-mounted cylindrical electron optics subsystems attached to the control electronics box (which is housed beneath the black multi-layer insulation (MLI) blankets). The curved aperture deflector plates, lying either side of the apertures themselves, can be seen through the entrance grid on both heads.

overview of the design, discuss the principles behind the making of the measurements before describing the details of some of the key and novel features of the design at subsystem level. We summarise the testing and calibration procedures that each of the hardware elements has undergone before summarising the design specification of each sensor as delivered to the spacecraft. In the case of the SWA-DPU, we also provide an overview of the software design and the on board scientific data processing algorithms.

3.1. The SWA Electrostatic Analyser System (SWA-EAS)

3.1.1. SWA-EAS introduction

To address the Solar Orbiter mission science goals, the SWA-EAS unit must be able to resolve the full 3D velocity space distributions of solar wind electrons with high cadence (<10 s time resolution). This basic measurement requirement can only be achieved by a sensor, or sensors, that have a combined FoV covering a large fraction of the 4π steradians of the full sky.

To achieve the requirement, the SWA-EAS consists of two identical top-hat electrostatic analysers, each with an aperture deflection plate system. Both are mounted on a common electronic box, which in turn is mounted at the end of a boom extending into the shadow of the spacecraft. Orthogonal mounting of the two sensor heads and an aperture deflection capability of ±45° on each head provides a full 4π FoV, with some degree of overlap and subject only to blockage by the spacecraft and its appendages.

With this deployment configuration, the expected FoV of the combined sensor system is as shown in Fig. 3. This shows the full sky FoV (±90° in elevation and ±180° in azimuth) with the Sun (and spacecraft) direction centred at (0,0). The blue grid represents the pixelated FoV of SWA-EAS head 1 (SWA-EAS1), while the red grid represents that of head 2 (SWA-EAS2). Some regions of sky are covered only by SWA-EAS1 or SWA-EAS2, while others are sampled by both heads. Sensor and spacecraft related blockages to the FoV are marked by the coloured regions, as described in the caption.

The sensor will measure electron fluxes and the SWA-DPU will calculate onboard and return moments of the electron distribution with a cadence of 4 s. In normal mode SWA-EAS will also return full 3D distributions at 100 s cadence. However, the sensor is capable of returning these at 1 s cadence where resources allow. The sensors will also provide 2D electron PADs at ~0.125 s cadence during short periods of burst mode. To achieve this at high cadence, the sensor will use information provided on board by the MAG sensor (Horbury et al. 2020) to steer the sensor look-direction using the aperture deflection system such that the unit samples only the plasma at elevations which contain the parallel and anti-parallel magnetic field directions. Since data is taken at all azimuth angles simultaneously, rebinning this data with respect to the magnetic field direction allows the assembly of a PAD in the time needed to perform two energy sweeps. This cadence has been selected to allow synchronisation with magnetometer data rates.

3.1.2. SWA-EAS design overview

The flight model (FM) configuration of the two SWA-EAS analyser heads and common electronics box is as shown in Fig. 4. Each head consists of three key modular sub-systems:

i. Electron optics (EO) system: consisting of the top-hat electrostatic analyser system (EA), aperture deflection system (ADS) and "top-cap" variable geometric factor system (VGFS);

ii. Detector and readout element: consisting of a microchannel plate (MCP) mounted onto an anode and readout board, including high-voltage (HV) coupling capacitors and readout electronics;

iii. EAS low voltage (LV) and HV distribution and control circuitry.

Sub-systems (i) and (ii) consist of a number of functional elements. Figure 5 shows a cross-section through a single analyser head and the location of the key functional elements, which are listed in the figure caption.

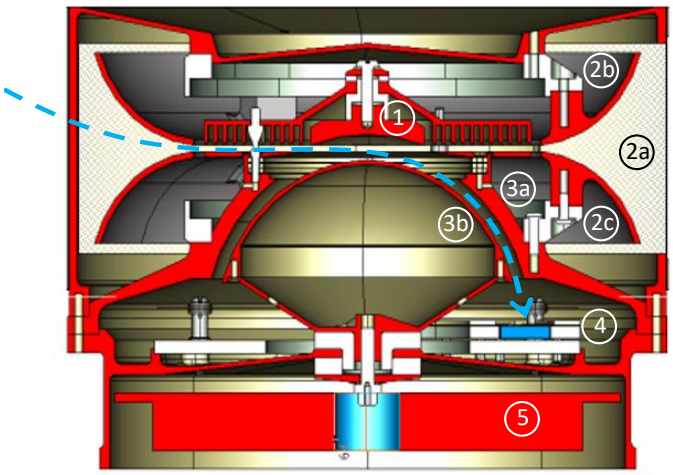

Fig. 5. Cross-section through a single SWA-EAS sensor head. Key subsystems are: (1) the VGF system "top-cap" anode; (2) (a) the entrance aperture shielding grid and (b,c) upper and lower plates of the deflection system; (3) (a,b) the upper and lower hemispheres of the electrostatic analyser; (4) the detector subsystem comprising a grid, the annular MCP, and the anode board, together with embedded HV coupling capacitors; (5) the application-specific integrated circuit (ASIC) 32 charge amplifiers. A representative electron trajectory through the sensor electron optics is shown by the blue dashed trace, for the case where the upper aperture deflection plate is charged positively.

Functional elements 1,2, and 3 form sub-system (i) and 4, 5, 6, and 7 form subsystem (ii). Provision of sub-systems (i) and (iii) are the responsibility of University College London's Mullard Space Science Laboratory (UCL MSSL) and sub-system (ii) is the responsibility of Laboratoire de Physique des Plasmas (LPP), Ecole Polytechnique, Palaiseau, France.

In addition, the electronics enclosure, also the responsibility of UCL MSSL, contains two identical sets of electronics boards independently servicing each of the analyser heads. These are the LV and HV electronics boards and the electronics boards hosting field-programmable gate arrays (FPGAs) for instrument control, interfaces, counters, electrical interfaces to the SWA-DPU, and the inter-experiment link (IEL).

3.1.3. SWA-EAS measurement principle

Solar wind electrons arriving at the spacecraft will enter one of the SWA-EAS sensor heads through the exterior shielding grid. The ADS uses positive voltages applied to either the upper or lower deflector electrodes, as needed, to steer electrons from a desired arrival direction into the EA section. The ADS acceptance angle can be varied through a range ±45° in 16 steps, requiring up to +2400 V on the deflector plates to accommodate the requirement for acceptance of up to 5 keV electrons at maximum deflection. The steps are selected to ensure continuous angular coverage while accounting for an increase in the acceptance angle resolution from ~2° to ~9° as the deflection angle increases. This ensures that any narrow (a few degrees) solar wind electron beams cannot fall between gaps in angular coverage and remain undetected. We note that although the deflector sweep voltages are symmetric in application, the response of the detector is asymmetric in terms of angular resolution for up and down sweeps. This is represented in the size of individual pixels shown in Fig. 3, and is discussed further in Sect. 3.1.6 below. The electrons then enter the hemispherical EA section, which permits only electrons of the selected energy to reach the detector subsystem. The design target k-factor, the ratio of the transmitted electron energy to the voltage applied between the hemispheres, is ~6.2, and the relative energy resolution is 13.5%. The maximum voltage on the inner hemisphere is +850 V. The azimuth acceptance angle of 360° for the EA is divided into 32 equal size bins, which allows determination of the electron arrival direction to within 11.25° in the detector plane. The combined ADS and EA component of each sensor thus samples the arrival direction of solar wind electrons over a 2.8π steradian solid angle range.

The 32 azimuth angle bins of each sensor head are all sampled simultaneously while the elevation angle bins must be sampled in their 16 steps sequentially by applying appropriate voltages to the upper or lower deflector plates. The sensor sweeps through 65 energy levels at each elevation, which was found to be the most efficient operation and also readily supports a scheme for tracking the magnetic field in the SWA-EAS burst mode (as detailed in Sect. 4.3.1). The usual cadence of the energy sweep is one sweep of 65 steps in 62.5 ms. Thus basic data accumulation time for any single energy-angle bin is ~0.92 ms. Combining the datasets from the two orthogonally-mounted sensor heads provides 4π steradian solid angle coverage (with 1.6π steradians in overlapping fields of view) and thus a complete measurement of the 3D VDF in $65 \times 16 \times 0.92$ ms ~ 1 s, although this is not the typically available down-linked time resolution of the VDFs.

The sensor unit is accommodated on the end of the boom in the spacecraft shadow, which both minimises the physical blockage of the spacecraft and its appendages on the SWA-EAS FoV and minimises the effect of spacecraft electrostatic interference in the measurement of the lowest-energy solar wind core electrons.

3.1.4. SWA-EAS design details

The overall functional block diagram for a single chain of the SWA-EAS unit is shown in Fig. 6. We now describe each of the key elements in that chain:

The SWA-EAS electron optics subsystem. The two annular curved deflection plates on each SWA-EAS analyser head steer incoming electrons into a hemispherical top-hat electrostatic analyser. The latter is of similar design to those flown on many previous missions (e.g. Carlson et al. 1982; Kessel et al. 1989; Johnstone et al. 1997; Carlson & McFadden 2013). Around the outside of the annular plates is wrapped a thin mesh designed to shield the incoming plasma from the voltages applied to the deflector plates. The design of the hemispherical analyser is derived from UCL MSSL heritage with instruments deployed on the Cluster, Cassini, and Double Star missions and uses parts which are precision-machined from aluminium alloy. The annular deflector plates are a new addition to this UCL-MSSL-built family of instruments and are supported on Vespel insulators to separate them electrically from the analyser top hat and the base plate. The top hat assembly is supported from the base plate by three pillars, (some of which are evident in Fig. 4). Co-aligned with the pillars are metal tubes that carry screened HV leads to the top hat assembly (also evident in Fig. 4). These support pillars are further co-aligned with anode gaps to minimise FoV loss and field distortion caused by the external and internal support pillars. The mesh is wrapped around the upper and lower end of the top and base plates. For radiation screening, the design aims to place a minimum of 2 mm of aluminium alloy around any critical instrument parts.

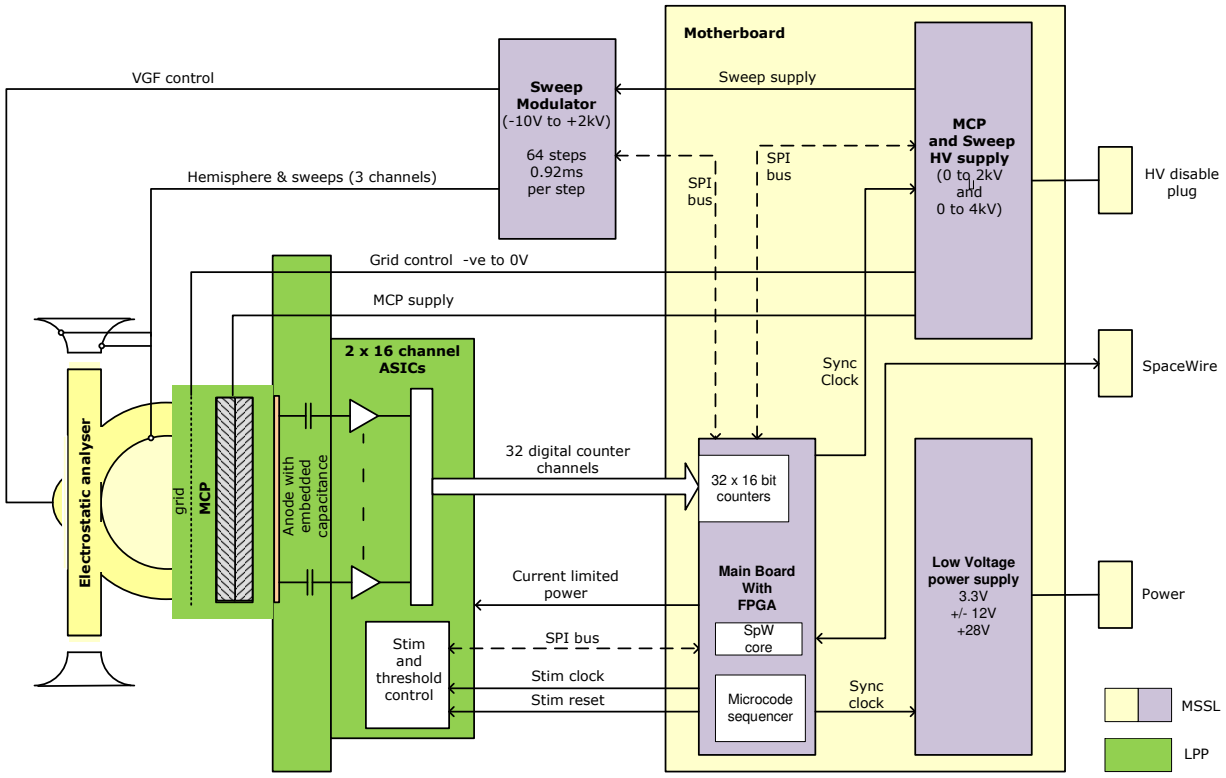

Fig. 6. Functional block diagram of single analyser head of SWA-EAS.

A second significant enhancement to the sensor heads over UCL MSSL heritage designs is the addition of a novel "top-cap" electrode, providing an electrostatic variable geometric factor (VGF) system (Collinson & Kataria 2010). The application of a commandable potential to the "top-cap" reduces the geometric factor of the system by restricting the fluxes of electrons that have passed through the ADS before they enter the EA. Addition of the VGF system increases the dynamic range of the instrument by up to two orders of magnitude, allowing the instrument to operate over the full range of solar wind conditions expected between 0.28 and >1 AU. This also provides a means to increase the lifetime of the detectors by reducing the total charge extracted from the MCPs.

Although most of the time the sensors should not be in direct sunlight, a UV photon and analyser internal photo-electron rejection scheme is required to deal with possible stray UV reflections from the spacecraft and occasional exposure to sunlight. This is achieved by use of a baffle system at the EA aperture and by use of Ebonol "C" coating for the non-reflective blacking of several internal parts. This coating also helps with trapping secondary electrons produced by energetic primary plasma electrons that contaminate the low energy end of the electron distributions. The coating produced by the Ebonol "C" process is jet black, chemically stable, heat stable, and very adherent. The finish itself will withstand temperatures up to ~190°C. This dual baffling and blackening approach has been used on previous similar flight instruments (specifically Cluster PEACE and Cassini ELS instruments) and has proven heritage.

EAS detector and readout electronics subsystem. The SWA-EAS Detector and Readout Electronics Subsystem is made up of a single printed circuit board (PCB) housed within each analyser head which also provides the MCP mount, the embedded HV coupling capacitors, and the MCP HV distribution circuitry. The detector block diagram is shown in Fig. 7. It is structurally based on an annular PCB with a circular array made up of 32 pixels printed on the top and the electronic circuitry associated with two ASICs and their associated discrete components on the bottom. A set of two annular circular MCPs of outside diameter 71.5 mm and centre hole diameter of 38.6 mm, stacked in a chevron assembly with a spacer of 50 μm between them, is positioned on the top face of the PCB. A front grid is then positioned on top of the MCP stack, with the assembly held together by a set of mechanical parts. The complete assembly, shown in Fig. 8, is then fitted in a circular housing within each analyser head. The mounting of the ASICs below the detector electronics and immediately beneath the MCPs, together with the shielding provided by housing the complete subsystem assembly in the lower part of the analyser head, is expected to provide a significant reduction of the radiation dose experienced by these sensitive components. A set of two identical such detector assemblies is needed to equip the two independent heads of the SWA-EAS.

The Anode board takes one HV input and divides the required voltages for the MCP and anodes internally. The thirty two anodes connect through small HV coupling capacitors embedded within the PCB to the two sixteen-channel ASICs containing the charge sensitive amplifiers (CSA) and leading edge discriminators. The detector PCB also receives interface commands via a dedicated Serial Peripheral Interface (SPI) bus from the SWA-EAS FPGA to configure the subsystem, including the threshold settings for the 32 CSA discriminators and a voltage (0 or −10 V) applied to the grid in front of the MCP for the rejection of low energy secondary electrons and UV induced photo-electrons. The LV connections are via a 51 way Omnetics bi-lobe nano-D type connector. The HV circuits are connected by a Reynolds HV coaxial connector.

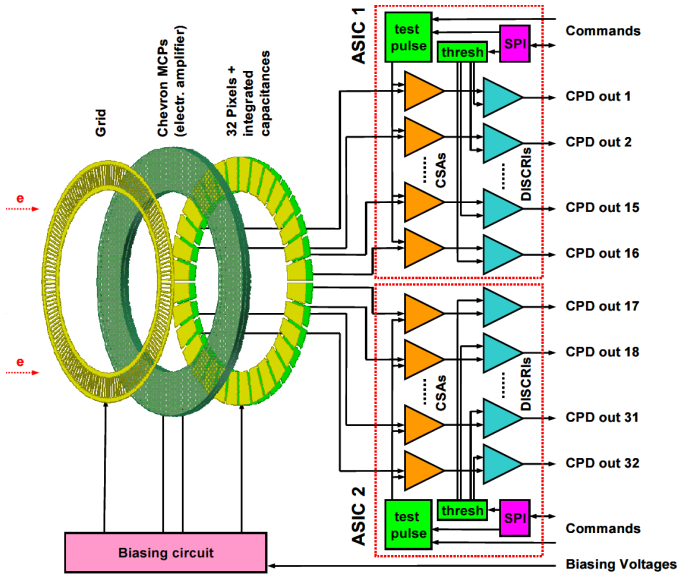

Fig. 7. EAS detector system block diagram.

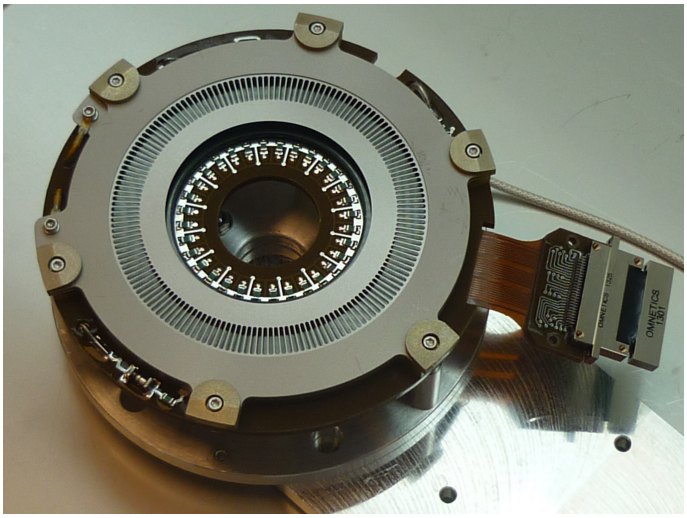

Fig. 8. EAS FM detector system.

The electrons arriving at the detector assembly through the analyser head electron optics pass through the front grid and enter the upper MCP, where they induce secondary electron emission through the micro-channels of the chevron MCPs. Electron clouds of $2-5\times10^6$ electrons (depending on the MCP voltage) are emitted from the rear of the lower MCP immediately below the impact point of the original electron, typically within a charge pulse lasting ~1 ns, and are collected on the anode. The amplitude of the associated voltage pulse generated depends on the impedance of the anode pixel and to the charge value. Due to the diameter of the charge cloud, a single electron impact may generate charge pulses on more than one anode pixels when the spot overlaps these two pixels. In addition, stray capacitances between pixels, may also generate pulses on the neighbouring pixels. To minimise this potential cross-talk, grounded tracks are placed between the anode pixels. Each one of the 32 anode pixels is connected to one of the input channels of the ASICs. Collected charges need to be in the range 16−2000 fC to match the dynamic input range of the CSAs. Charge pulse heights are assessed against the threshold applied to the 32 discriminators. These thresholds can be independently adjusted to discriminate only the main charge pulses but not the secondary charge pulses due to capacitive cross-talk. Output signals from the 32 channels which exceed the associated thresholds are then supplied to the FPGA via the motherboard as a count of the electrons arriving at each azimuth pixel of the detector during each energy-elevation angle accumulation period.

EAS HV sweep modulator subsystem. An HV sweep modulator PCB is mounted on the back of each analyser head and is connected to the electronics box via Reynolds HV coaxial connectors to enable each analyser head assembly to be readily removed as a complete testable unit. This HV sweep modulator board takes a single static HV supply at 2015 V from the Sweep HV Supply board and generates four scanning HV outputs which have high slew rates, low noise, and fast settling times. The modulator uses opto-couplers from Micropac which have been qualified for space and military use. The four outputs are assigned to the following electrodes: upper deflector plate, lower deflector plate, VGF, and inner hemisphere. The HV levels are controlled by the SWA-EAS FPGA (see below) via four SPI control busses. The subsystem uses two 12-bit digital-to-analogue converters (DACs) per channel to define the required HV levels for each sensor head subsystem. These are combined to give 20 bits of resolution with the output voltage per bit being ~1.6 mV with the smallest required step difference of ~10 mV. The maximum HV output is set to 1990 V and the minimum is ~−13 V. Read back of these voltages is provided via its housekeeping (HK) SPI to the main SWA-EAS electronics board under control of the FPGA's HK system. The LV connections are via a 31 way Omnetics bi-lobe nano-D type connector. The HV is transmitted from the HV supply by a Reynolds HV coaxial connector. The four HVs to the analyser are also transmitted via Reynolds HV coaxial connectors. The mounting of each of the analyser heads directly on to the electronics box case provides a compact unit of minimum mass with the shortest possible connections between the electronics and each analyser.

EAS LV and HV distribution and control subsystems. The remaining PCBs for each sensor head are housed in the SWA-EAS electronics box forming rear part of the structure as seen in Fig. 4. For ease of cable and connector routing and access, the PCBs for each sensor head are housed on the opposite side of the electronics box structure to that on which the related head is mounted. The forward part of the structure ahead of the front bulkhead is occupied by the cables and connectors.

To meet the minimum 2 mm structure screening thickness, the electronics case is a mixture of parts machined from both solid and sheet metal. The spacecraft boom fixing is via four threaded holes, two in each of the front and rear bulkheads with clearance holes in the top structure plate to enable the top face of the SWA-EAS to be bolted to the boom flange with thermal control bushes between them. Interface connectors are grouped in analyser sets on the rear bulkhead and a single purge connector feeds both analysers via an internal "Tee" piece. A heater interface bracket and instrument earthing stud are also positioned on the rear bulkhead.

In addition to the anode board mounted in the analyser head itself and the sweep modulator board mounted on the rear of the analyser head (both described above), the system consists of four other boards: The MCP and sweep HV supply board;

the SWA-EAS main board; and the Low Voltage Power board; these are each hosted by the fourth board, the motherboard, and are mounted within the electronics enclosure. The three motherboard mounted PCBs connect to the sweep modulator PCB, the anode PCB, and the SWA-DPU via connectors on flying leads soldered to the mother board. The exceptions are the two HV supplies, which connect to the MCP and sweep HV supply PCB via HV Reynolds connectors.

The MCP and sweep HV supply board produces one programmable HV, one static HV, and an auxiliary −30 V output. It also generates the 0 V to −8 V variable output supply for the grid in front of the MCP using a single 12-bit DAC and an op-amp to produce this output. The static HV output of ∼2 keV and auxiliary −30 V output are used to supply the sweep modulator board with a raw HV, while the other controllable output is variable between 0 V and +3700 V and supplies the MCP. This output has ripple <0.1% over the MCP operational output voltage range. The MCP voltage is controlled by SWA-DPU command over the SpaceWire (SpW) link via the SWA-EAS main board. It takes a 10 kHz clock from the main board, and uses alternate edges to synchronise the two converters, thus giving 20 kHz as its fundamental switching frequency.

The SWA-EAS main board hosts the system master crystal oscillator, supplying the 19.98848 MHz system clock, which in turn is used to synchronise all power conversion. This board also hosts the FPGA and the SpW low voltage differential signalling (LVDS) drivers and receivers. The FPGA is the master controller for SWA-EAS and provides all control of: data acquisition; HV scanning and other instrument timing, performed by a sequencer which uses an uploaded "sequence table" to control SWA-EAS; SWA-DPU communication including housekeeping, science data, and commanding (including command parsing and checking); HV and LV power supply synchronisation; the time control system; and active thermal control for the operational heater(s). The SWA-EAS main board also supports SWA-EAS sensor communication with the SWA-DPU via SpW at 10 Mbits s^{-1}. We note in passing that the FPGA design deployed for SWA-EAS also supports, without modification, the operation of the SWA-PAS unit (see Sect. 3.3.2).

The Low Voltage Power Board is designed to take switched bus power from the SWA-DPU and provide ±8.5 V, 10 V, 28 V, and 3.3 V isolated supplies to the rest of SWA-EAS. It is synchronised by the FPGA to 294 ∼ 300 kHz.

Finally, the SWA-EAS mother board provides a back plane and host for connections to other SWA-EAS electronics boards and to the SWA-DPU. It provides the low voltage and logic connections between the low voltage power board, the SWA-EAS main board, and the HV supply board. It also has the low voltage connectors for the 28 V power input, the SpW interface, the HV enable plug, and the two bi-lobe connectors to the sweep modulator and anode PCBs. It also accommodates opto-isolation for the heater control. The mother board uses the Hypertac CSD family of four row connectors for PCB interconnect. The SWA-EAS internal power returns are connected to the structure at the anode PCB. The incoming power bus return is not connected to the structure at SWA-EAS.

3.1.5. SW-EAS testing, characterisation, and calibration

The SWA-EAS instrument has been integrated and calibrated in a number of different phases. In the first phase, MCP preselection and characterisation of the MCPs were carried out at LPP, followed by characterisation and performance of the integrated detector and readout subsystem. This included a detailed characterisation of the front-end readout ASICs and a determination of temperature response of the subsystem.

Following the integration of the full SWA-EAS FM, the primary phase of the FM calibration activity was carried out at UCL MSSL, where a full calibration of both SWA-EAS sensor heads was performed using dedicated electrical ground support equipment (EGSE) to rotate the sensor within an electron beam of known energy set up in the laboratory's LEPIC (Low Energy Plasma Instrument Calibration) vacuum chamber. The purpose of this activity was to determine the sensor performance parameters, including the sensor k-factors, relative geometric factors, and the energy and angular response. These parameters must be determined for the large parameter space covered by the combination of the energy selection performed by the inner hemisphere, the look-angle selection performed by the ADS, and the geometric factor selection performed by the VGF system.

This FM sensor was bombarded by the known energy beam while performing voltage-elevation scans at various azimuth angles. For the voltage-elevation scans, the instrument is rotated to a chosen azimuth angle and set for different voltages. The number of transmitted particles at each voltage (equivalent to energy) is then recorded for an elevation angle and the process is repeated for the range of elevation angles so as to cover the full energy-elevation parameter space. The process is then repeated at all the required azimuth positions. Moreover, three sets of energy-elevation scans are carried out. First, voltage is applied to the inner hemisphere only (with elevation angle range confined typically to ±5° (for energies >100 eV) or ±10° (energies <100 eV)). Then voltages are applied to both the inner hemisphere and deflector plates, and finally to each of the inner hemisphere, deflector plates, and variable geometric factor system. In the latter two sets of tests the elevation angle range was typically ±50°, that is to say beyond the required ±45° for each sensor head. In a majority of the tests, the azimuth angles were chosen so that the beam was incident on the centre of each of the anodes. The voltage range was typically chosen to permit transmission of ±12% of the set energy.

The response of the unit to secondary electron contamination was assessed during the calibration activity and found to be satisfactory (<2% contamination level). A number of other tests, including cross-calibration of the two SWA-EAS sensor heads, determining the efficiency of UV stray light rejection, and the potential thermal drifts in the HV modulators, will be completed in flight and with reference laboratory tests performed on the flight spare.

EAS in-flight calibration. The evolution of MCP sensitivity (or "gain") as a function of applied HV can be monitored using periodic tests in which one of the two SWA-EAS sensors is operated normally while the MCP voltage on the other is slowly raised from a low level. The use of two SWA-EAS identical sensors allows a normalisation that isolates count rate changes due to MCP voltage changes from those due to changing solar wind conditions. This technique has been developed at UCL MSSL and used successfully on the Cluster PEACE instruments. The relative calibration of different parts of the MCP is very important, especially for deriving moments of the measured electron VDFs, and it will be monitored using well-established technique based on long-term symmetries in the distributions. Inter-experiment cross-calibration between the SWA experiments and between SWA and the plasma wave instrument RPW (Maksimovic et al. 2020) are envisaged in order to refine the geometric factor and directional response knowledge on all sensors, verifying and improving ground calibration knowledge.

Table 1. Summary of SWA-EAS design and build and ground calibration results for FM SWA-EAS heads.

Parameter	Range and resolution	EAS design goal	EAS build and calibration
Sensors		2 × EA	2 × EA
Mass	Species	Electrons	Electrons
Energy	Range	1 eV–5 keV	1 eV–5 keV
	Energy scan	64 steps	64 steps
	Resolution ($\Delta E/E$)	12%	13%
	Analyser constant (eV/V)	6	~6.65 (SWA-EAS1) ~6.30 (SWA-EAS2)
Angle	Range (AZ)	360°	360°
	Range (EL)	±45°	±45°
	Range scan (EL)	16 steps	16 steps
	Resolution (AZ × EL)	11.25° × 3°–8°	11.25° × 6°–12°
	Pixel FoV	11.25° × 3°–8°	11.25° × 6°–12°
Temporal	Basic accumulation period	0.96 ms	0.96 ms
	Normal mode	4 s moments	1 s moments every 4 s or 4 s moments
		100 s full 3D VDFs	1 s full 3D VDFs every 100 s (or every 400 s or every 10 s)
	Burst mode	0.125 s p.a.d.	0.125 s p.a.d.
	Triggered mode	1 s full VDF every 1 s for 5 min	1 s full VDF every 1 s for 5 min
Sensitivity	Per pixel (cm^2 sr eV/eV)	Variable, ≥8.0×10^{-5}	Variable, 8.0×10^{-5} for pixels with clear FoV

3.1.6. Summary of SWA-EAS specifications at delivery

A summary of the design goals versus the achieved characteristics of the two SWA-EAS sensor heads is given in Table 1. Overall, the performance is close to that expected on the basis of the design and simulations. The energy resolution is ~13% and the two heads show only a small difference in their analyser constant, k.

The performance in elevation angle resolution has an unusual energy dependent variation. Figure 9 illustrates the elevation angle performance of the two FM sensor heads (SWA-EAS1 in left column, SWA-EAS2 in right). The top row shows the bandwidth of each of the 16 elevation settings for the sensor head (coloured traces) and the overall passband (black line). The second row then shows the response for the peak of the transmitted elevation angle distribution as a function of the voltage applied to the aperture deflection system (ratio as a function of inner hemisphere voltage). An asymmetry in the positive-negative deflection angles is observed, consistent with the charged particle optics simulations of the sensor design. The plots in the lower row show the width of the transmitted elevation angle distribution for each elevation setting (FWHM of the passbands in the upper plots). There is a variation in the acceptance angle ranging from ~6° to ~13°. This is higher than the ~2° to ~9° observed in calibrations at higher energies, typically above 1500 eV, and predicted by the simulations. Below 1500 V, the width increases from ~2° up to ~6° as the calibration energy is lowered to below 30 eV. This energy dependent behaviour is under investigation at the time of writing this paper. The most likely explanation is a broadening of the incident beam itself at lower energies. However, if the energy dependence is found to be intrinsic to the sensor response, for example, due to stray electrostatic fields not accounted for in the simulations or increased elastic scattering within the sensor apertures at low energies, this will have to be accounted for in on-board and ground calibration parameters.

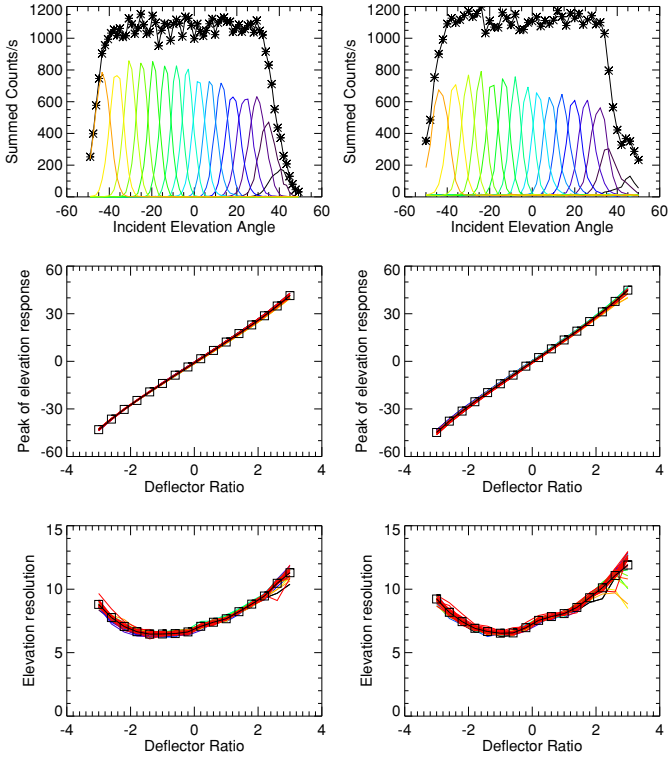

Fig. 9. Elevation response of FM SWA-EAS sensors heads (SWA-EAS1 in *left column*, SWA-EAS2 in *right column*). *Top row*: counts received in each sensor elevation bin as a function of the elevation angle of the incident electron beam. *Second row*: elevation angle showing peak response as a function of the voltage ratio applied to the deflectors, showing good linearity. *Bottom row*: FWHM of the response angle as a function of the voltage ratio, indicating that there is an asymmetry in the response for "upward" and "downward" sweeps and that the acceptance angle is larger at larger deflections.

Overall, the SWA-EAS sensor will be capable of measuring the full 3D VDF of electrons in the energy range 1 eV–5 keV with a cadence of 1 s, with measurements of a 2D pitch angle sample at 0.125 s cadence. This covers the core, halo, and strahl components of the overall solar wind electron population with high resolutions in time, energy, and angular acceptance. Due to telemetry restrictions, these data must be processed on board to form moments of the electron distribution which will be added to the telemetry stream every 4 s, or returned in their raw form only sporadically. Full 3D VDFs will be routinely returned at a nominal cadence of 100 s, but can also be returned at faster or slower rates depending on the telemetry constraints. Full-time resolution 3D VDFs will also be returned in short (~5 min) periods following occasional response to a triggered event (Walsh et al. 2020). The 2D pitch angle data will also be returned from short (5–10 min) periods of burst mode activation.

3.2. The SWA Heavy Ion Sensor (SWA-HIS)

3.2.1. SWA-HIS introduction

In support of the Solar Orbiter mission science goals, SWA-HIS will measure heavy ion composition and kinetic properties from solar wind up through suprathermal energies. To achieve these science goals, SWA-HIS must address two fundamentally different sets of measurement objectives. First, it must measure the ion and elemental composition and 3D VDFs of heavy ions (He–Fe) in the bulk solar wind between 0.5 and 18 keV/e.

Second, it must measure the ion and elemental composition and 3D VDFs of the major constituents: He, C, O, and Fe in the suprathermal energy range up to 60 keV/e. To achieve the characterisation of 3D VDFs for these populations, SWA-HIS is mounted within a cut-out in the corner of the spacecraft heat shield, with its FoV facing the solar direction. It has a FoV that spans a native 96° in the ecliptic from −30° off the Sun-Spacecraft line to +66° off the Sun-spacecraft line to account for the aberration of the solar wind due to motion of the spacecraft, and to allow for improved sampling of suprathermal and pickup ions. SWA-HIS scans through ±17° above and below the ecliptic. SWA-HIS will measure alpha particle and heavy ion 3D VDFs in solar wind, pickup ion, and suprathermal energy ranges, with native time resolution as high as 4 s in Burst Mode, 30 s in Normal Mode, and 300 s for Normal Mode (Low Cadence). This time resolution corresponds to the time it takes to scan the entire energy range from 0.5−80 keV/e in 64 steps, and sample all elevation angles in 16 steps. SWA-HIS will return a number of heavy ion rates, onboard calculated VDFs, and a statistically representative sampling of Pulse Height Analysis (PHA) event words to reconstruct high fidelity 3D VDFs of all heavy ions. From these 3D VDFs, SWA-HIS will provide measurements of elemental abundances and charge state distributions of He, C, O, Mg, Si, and Fe. SWA-HIS will provide the first-ever solar wind and suprathermal heavy ion composition measurements in the inner heliosphere.

3.2.2. SWA-HIS design overview

Figure 10 shows a photograph (left) and computer-aided design (CAD) model (right) showing a complete overview of the mechanical sections of SWA-HIS. Due to its exposure to the Sun, SWA-HIS includes its own heat shield, which wraps around the entrance system, as seen in the photograph. The aperture of the instrument is a narrow slit in the instrument heat shield, behind which the SWA-HIS pairs an electrostatic analyser (EA) with entry ion steering (IS) to form (right-upper) the upper EA-IS subsystem, which will optimise the out-of- ecliptic particle sampling. The bottom of the EA-IS is mated to a grounded housing (right middle) containing an isolated time of flight (TOF) telescope and associated electronics. The heat shield, EA-IS, and grounded housing containing the TOF telescope are mounted on top of the main electronics (ME) box (right-lower), which contains the low-voltage power supply (LVPS), post-acceleration (PA) high-voltage power supply (HVPS), and associated boards.

SWA-HIS EA-IS system. The SWA-HIS entrance system is comprised of a top-hat hemispherical EA paired with IS plates behind the entrance aperture in the instrument heat shield. The ion steering plates include top and bottom deflectors as well as a "top-cap" deflector; these deflectors steer ions in through the entrance aperture from above and below the ecliptic. Ions can be steered ±17° in the polar direction, above and below the aperture.

HIS TOF telescope. The TOF telescope measures time-of-flight and total kinetic energy of incoming ions. When paired with the EA-IS, this provides optimum separation of incoming ions by energy, mass, and charge. The TOF telescope is floated at −25 keV, supplied by the PA HVPS, which is housed in the ME box. The TOF telescope is isolated from the grounded housing by the PA vacuum gap shown in Fig. 10 (right). The TOF telescope also includes a carbon foil (CF) entrance window, MCPs paired with position sensing readout anodes, and an array of solid state detectors (SSDs), and all of the associated electronics.

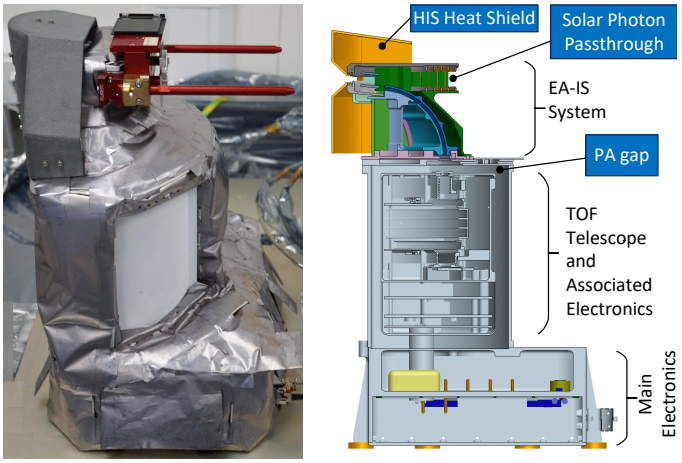

Fig. 10. *Left*: photograph of SWA-HIS in "as delivered" configuration. *Right*: schematic showing the different SWA-HIS building blocks.

The isolated detector section (DS) data interface is located in the TOF telescope.

HIS ME box. The ME box includes the PA-HVPS, the detector section LVPS, the ground side of the data interface with the TOF telescope, the EA-IS HVPS, the C&DH board, and the instrument LVPS. The C&DH board runs the flight software, which controls most aspects of the sensor.

3.2.3. SWA-HIS measurement principle

SWA-HIS requirements demand the derivation of five key properties from the measurements of all ions: mass (m), charge (q), speed (v), and direction of incidence, elevation (θ) (above and below aperture, in the polar direction), and azimuth (ϕ) (along the entrance aperture, nominally in the ecliptic). SWA-HIS provides these properties as follows: SWA-HIS EA-IS provides E/q and θ information. SWA-HIS TOF provides the ϕ information through both the SSD ID, and through the imaging of secondary electrons on the Start MCP anode, generated as the ion passes through a thin carbon foil at the entrance of the TOF telescope. These secondary electrons also serve to start the timing window for TOF (τ) measurement when they impact the Start MCP. To push solar wind ions above the SSD energy threshold, the TOF telescope floats at a potential of −25 keV. This potential accelerates the incoming solar wind ions so that their detection efficiencies are almost independent of their initial speed. Once the ion impacts the SSD, secondary electrons are emitted and steered to the Stop MCP for closure of the timing window, from which the speed of the ion within the TOF chamber can be determined. The SSD measures the total energy of the accelerated ion ($E_{\rm Tot}$). Combining E/q, τ, and $E_{\rm Tot}$ enable the calculation of ion's mass, charge, and velocity (e.g. Shearer et al. 2014). Angles of incidence are obtained as described above. This completes the five independent measurements required for unique ion identification and characterisation.

The conceptual design of the SWA-HIS EA-IS is driven by requirements that major heavy ion species should be measured up to energies of 60 keV/e ($\Delta E/E \leq 10\%$), and a maximum time resolution of 4 s for alpha particles and 30 s for heavy ions. The FoV of the instrument ranges from −33° to +66° in the azimuthal (ecliptic plane), and ±17° in the polar directions for optimum sampling of the solar wind ions, pickup ions, and suprathermal